Proceedings of the 9th International Conference on Fluid Flow, Heat and Mass Transfer (FFHMT'22)
Niagara Falls, Canada – June 08-10, 2022
Paper No. 206
DOI: 10.11159/ffhmt22.206

Ansys Fluent Automation for Fluid Flow and Heat Transfer in Corrugated Channels

Mohamed Shaimi[1], Rabha Khatyr[2], Jaafar Khalid Naciri[3]
Laboratory of mechanics, Faculty of Sciences Aïn Chock, Hassan II University of Casablanca
Km 8 Route d'El Jadida, B.P 5366 Maarif 20100, Casablanca 20000, Morocco
[1] mohamed.shaimi-etu@etu.univh2c.ma ; [2] khatyrrabha@gmail.com ; [3] naciriuh2c@gmail.com

Abstract **–** This paper presents an original numerical study for the optimization of the steady laminar fluid flow and heat transfer in a two-dimensional corrugated channel with a bottom heated wall and an upper periodically corrugated wall. A python code is used to automate Ansys Fluent and to run the simulation for various shapes of the corrugated wall given by a polynomial function. The optimal values for the coefficients of the fifth-order polynomial defining the shape of the upper wall are determined. The average Nusselt number and the Reynolds number are plotted as a function of two geometrical coefficients. A correlation for the average Nusselt number as a function of the Reynolds number for this flow is proposed. It was found that there exist optimal parameters of the corrugated channel for which the average Nusselt number is higher than that of parallel walls due to the development of secondary flows.

Keywords**:** Fluid Flow, Heat Transfer, Corrugated Channel, Ansys Fluent Automation, Python Scripting

1. Introduction

There is an increasing need for better use of energy in its different forms and this is for reasons of an industrial, financial, and environmental nature. Among the concerned areas, the improvement of thermal performances of heat exchangers can contribute significantly to increasing the efficiency of energy use in different industrial areas where heat exchangers are an essential component such as air conditioning, electronic components cooling, and other fields [1-8]. The corrugated channels are one of the passive flow control techniques used in industrial heat exchangers to improve their thermal performances.

Several investigations have been made on the heat transfer enhancement in corrugated channels. Wang and Vanka [9] numerically investigated the convective heat transfer in periodic sinusoidal wavy channels. Fabbri [10] studied numerically the steady laminar flow and heat transfer in a corrugated channel using the finite element method. The channel is composed of a flat wall and a periodically corrugated wall with non-negligible thickness. The heat transfer was maximized by optimizing the wall corrugation profile, which is given by a fifth-order polynomial function, using a genetic algorithm under constant pressure drop and constant volume. Later, Fabbri and Rossi [11] used an optimized corrugated channel for the analysis of the heat transfer in the entrance region. Naphon [12] studied numerically the effect of wavy plate geometry configurations on the velocity and temperature distributions. Recently, Kurtulmuş and Sahin [13] presented a review of the various investigations in the literature on the flow and heat transfer in corrugated channels of different design parameters using analytical, numerical, and experimental methods.

In this paper, the objective is the development of a new original Python code that automates Ansys Fluent and allows systematizing the thermal optimization of the flows in channels with corrugated walls. The code will be used to carry out a study on the steady laminar fluid flow and heat transfer in a two-dimensional corrugated channel. Unlike the various investigations in the literature where the corrugation is used on the heated wall, the corrugation in this paper is used on the thermally insulated wall. The periodic corrugated upper wall is thermally insulated and uniform heat flux is imposed on the bottom flat wall. The corrugated profile is given by a polynomial function and the average Nusselt number is calculated for different values of the geometrical coefficients. A correlation for the average Nusselt number as a function of the Reynolds number is determined.

2. Methodology

Computational Fluid Dynamics (CFD) simulations are widely carried out using Ansys Fluent among researchers and industrials. The Graphical User Interfaces (GUI) of the programs can be used to run the simulation but it is also possible to

use Text-based User Interfaces (TUI) which provide flexibility and more control over the simulation especially when similar simulations are to be run more than once. The use of Application Programming Interfaces (API) allows external communications with different programming languages and programs.

2.1. Geometry Configuration

Figure 1 shows the two-dimensional periodic corrugated channel that is composed of a flat wall at $y = 0$ and a periodically corrugated wall given, for $0 \leq x \leq L$, by a polynomial function $f(x)$ which is written as:

$$y = f(x) = \sum_{i=0}^{N} a_i \left(\frac{x}{L}\right)^i \tag{1}$$

where N is the order of the polynomial function, L is a characteristic length (the length of one period), and $\{a_i\}$ are constant coefficients that define the corrugated profile and are compatible with imposed geometric constraints specified in what follows.

The rest of the periodic channel are determined using a translation by a number of periods, for example, the corrugated profile for $\omega L \leq x \leq (\omega + 1)L$ is given by $f(x - \omega L)$ where ω is an integer.

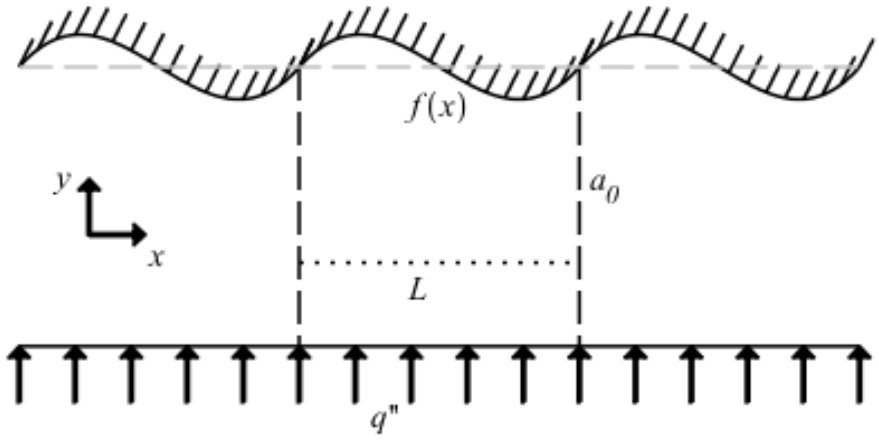

Fig. 1: Two-dimensional periodic corrugated channel.

The first constraint is that the volume of the fluid domain is constant, which is expressed by the following equation:

$$V = \int_0^L \int_0^{f(x)} dy\, dx = \sum_{i=0}^{N} \frac{a_i L}{i+1} = constant \tag{2}$$

The constant volume can be chosen as the volume of the rectangle with the length L and the height $a_0 = f(x = 0)$ (height of the inlet surface of the period between $x = 0$ and $x = L$) that will be fixed for all the different geometrical configurations. Therefore, Eq. (2) becomes:

$$\sum_{i=1}^{N} \frac{a_i}{i+1} = 0 \tag{3}$$

The second constraint is that the inlet surface and outlet surface of the period between $x = 0$ and $x = L$ are equal, $f(x = 0) = f(x = L)$, which leads to the following constraint on the coefficients:

$$\sum_{i=1}^{N} a_i = 0 \tag{4}$$

The third constraint is that the first derivation of the function $f(x)$ at the inlet and outlet of the period between $x = 0$ and $x = L$ are equal, $\frac{df}{dx}\Big|_{x=0} = \frac{df}{dx}\Big|_{x=L}$, which leads to the following equation:

$$\sum_{i=2}^{N} i a_i = 0 \tag{5}$$

The fourth constraint is that the fluid domain is between the lower and upper walls so the function $f(x)$ is bounded by the lower flat wall. Thus, the following constraints are imposed to prevent the channel from being too narrow:

$$\min_{0 \le x \le L} f(x) > (1 - \varepsilon) a_0 \tag{6}$$

$$\max_{0 \le x \le L} f(x) < (1 + \varepsilon) a_0 \tag{7}$$

where ε is a percentage between 0 and 1 that specifies the limits of the fluid domain as compared to the reference height a_0.

Ansys Space Claim is used to create the geometry and the named selections so that they can be recalled later in the meshing and the definition of the boundary conditions. The use of Python scripting allows the introduction of the different coefficients $\{a_i\}$ explicitly as input parameters of the study.

2.2. Governing Equations

The steady laminar incompressible flow of a Newtonian fluid with constant thermophysical properties is governed by the mass conservation equation, the momentum conservation equations, and the energy equation. These equations under the assumptions used in this study, namely negligible body forces and viscous dissipation, are written in the cartesian coordinates for a 2D model as:

$$\frac{\partial u}{\partial x} + \frac{\partial \mathrm{v}}{\partial y} = 0 \tag{8}$$

$$\rho\left(u\frac{\partial u}{\partial x} + \mathrm{v}\frac{\partial u}{\partial y}\right) = -\frac{\partial p}{\partial x} + \mu\left(\frac{\partial^2 u}{\partial x^2} + \frac{\partial^2 u}{\partial y^2}\right) \tag{9}$$

$$\rho\left(u\frac{\partial \mathrm{v}}{\partial x} + \mathrm{v}\frac{\partial \mathrm{v}}{\partial y}\right) = -\frac{\partial p}{\partial y} + \mu\left(\frac{\partial^2 \mathrm{v}}{\partial x^2} + \frac{\partial^2 \mathrm{v}}{\partial y^2}\right) \tag{10}$$

$$\rho C_p\left(u\frac{\partial T}{\partial x} + \mathrm{v}\frac{\partial T}{\partial y}\right) = k\left(\frac{\partial^2 T}{\partial x^2} + \frac{\partial^2 T}{\partial y^2}\right) \tag{11}$$

where ρ, μ, C_p, k, p, and T are respectively the density, the viscosity, the specific heat, the thermal conductivity, the pressure, and the temperature of the fluid, and u and v are respectively the velocity components in the x- and y- directions.

2.3. Boundary Conditions

The boundary conditions for the velocity are given by the no-slip condition at the channel's walls. They are written respectively at the bottom and upper walls as:

$$u(x, y = 0) = \mathrm{v}(x, y = 0) = 0 \tag{12}$$

$$u\big(x, y = f(x)\big) = \mathrm{v}\big(x, y = f(x)\big) = 0 \tag{13}$$

The upper wall is adiabatic (null heat flux) and uniform heat flux, q'', is imposed on the bottom wall.

A periodic hydrodynamically and thermally fully developed flow regime is considered so that the inlet and outlet of the period between $x = 0$ and $x = L$ are matched with the periodic conditions and only one period is enough to carry out the study, which reduces the computational time. The following equations represent the periodic condition:

$$u(x, y) = u(x + L, y) \tag{14}$$

$$\mathrm{v}(x, y) = \mathrm{v}(x + L, y) \tag{15}$$

$$p(x, y) = p(x + L, y) + \Delta p \tag{16}$$

$$T(x, y) = T(x + L, y) + \Delta T \tag{17}$$

where, Δp is the constant pressure drop across the period along the streamwise direction, and ΔT is given by:

$$\Delta T = T_{bulk,outlet} - T_{bulk,inlet} \tag{18}$$

where, $T_{bulk,inlet}$ is the known inlet bulk temperature.

2.4. Output Parameters

The power cost is constant due to the use of constant total heat flux on the bottom flat wall and constant pumping power. The total heat flux on the bottom flat wall is constant because the length of that wall is unchanging for all the different geometrical configurations. The pumping power is constant because of the constant pressure drop along the streamwise direction and the geometrical constraints presented in subsection 2.1. So, thermal performances of the different corrugated profiles can be evaluated using the average Nusselt number Nu_a which is given by:

$$Nu_a = \frac{1}{L}\int_0^L Nu(x)dx \tag{19}$$

The average Nusselt number will be used as an output parameter and the integral will be calculated numerically using a Simpson method.

The local Nusselt number $Nu(x)$ at the bottom flat wall is given by:

$$Nu(x) = \frac{h(x)D_h}{k} \tag{20}$$

where $D_h = \frac{4V}{A}$ is the hydraulic diameter [5,6], V and A are respectively the volume of the fluid domain and the area of the wetted walls. The local convective heat transfer coefficient $h(x)$ is given by:

$$h(x) = \frac{q''}{T_w(x) - T_b(x)} \tag{21}$$

where q'' and $T_w(x)$ are respectively the uniform heat flux and the temperature at the bottom flat wall, and $T_b(x)$ is the bulk temperature at section x which is given by:

$$T_b(x) = \frac{\int_0^{f(x)} u(x,y)T(x,y)dy}{\int_0^{f(x)} u(x,y)dy} \tag{22}$$

The second output parameter of the study is the Reynolds number Re which is given by:

$$Re = \frac{\rho U_0 D_h}{\mu} \tag{23}$$

where, $U_0 = \frac{Q}{a_0}$ is a characteristic velocity and Q is the flow rate.

3. Results and Discussions

The corrugated profile is given by a fifth-order polynomial function $f(x)$ where the coefficients $\{a_i\}$, considering the geometrical constraints imposed on them in subsection 2.1, are given by:

$$a_0 = \alpha L; \quad a_1 = \frac{a}{2} + \frac{2b}{5}; \quad a_2 = -\frac{3a}{2} - b; \quad a_3 = a; \quad a_4 = b; \quad a_5 = -\frac{2b}{5} \tag{24}$$

where a and b (respectively a_3 and a_4) are two geometrical coefficients that define the different corrugated profiles. The other coefficients $\{a_1, a_2, a_5\}$ are fixed by using Eqs. (3) – (5). The coefficients a and b will be varied in the range between $-3L$ and $3L$ with a step equal to L. This leads to 49 different configurations which means 49 different simulations that will be run by using Ansys Fluent automation. α is a constant coefficient that defines the ratio between the height of the inlet and the length of the period which is chosen to be equal to the unity for the current case studied. Figure 2 shows a sample of the corrugated profiles for $\frac{a}{L} = -3$ and $\frac{b}{L} = -3, -1, 1, 3$. The percentage ε for these 49 configurations is equal to 0.3 which means from Eqs. (6) and (7) that $0.7a_0 < f(x) < 1.3a_0$ for $0 \leq x \leq L$.

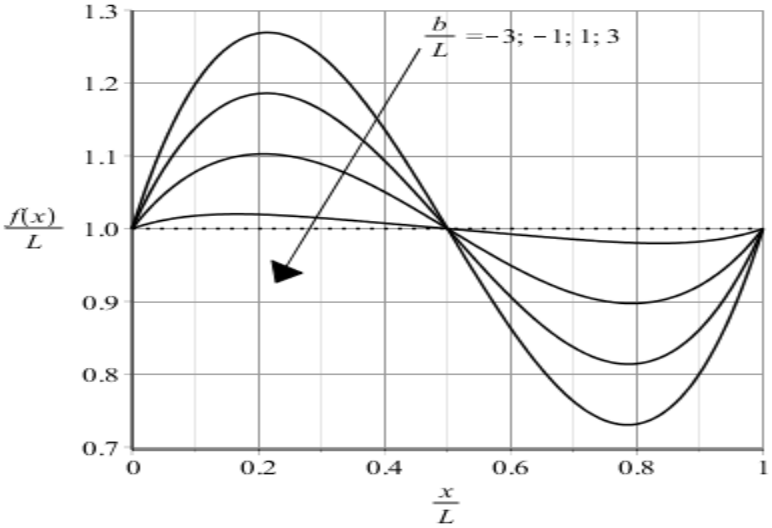

Fig. 2: The corrugated profiles for $\frac{a}{L} = -3$ and $\frac{b}{L} = -3, -1, 1, 3$.

Figures 3 and 4 show respectively the average Nusselt number and the Reynolds number as a function of the two coefficients $\frac{a}{L}$ and $\frac{b}{L}$. The deformation of the upper wall increases its length which induces an increase in the contact surface between the fluid and the upper wall and therefore the flow resistance increases due to the fluid friction at the walls. Thus, the flow rate drops, and therefore the Reynolds number decreases as can be seen from Figure 4. The average Nusselt number decreases as well when the Reynolds number decreases due to the decrease in the flow rate which means lower convective heat transfer. However, there exist optimal parameters for which the average Nusselt number values are higher than the case of parallel walls as can be seen from Figure 3. This is due to the secondary flows that appear in the case of corrugated walls which bring cooler and hotter chunks of the fluid into contact leading to higher rates of conduction at a much larger number of sites in the fluid. The optimal corrugated profiles correspond to the geometrical coefficients that satisfy the following equations:

$$b = -a - 2L \tag{25}$$

$$b = -a + 2L \tag{26}$$

The solutions are symmetric with respect to the point $a = b = 0$ because the corresponding corrugated profiles are only translated by half period.

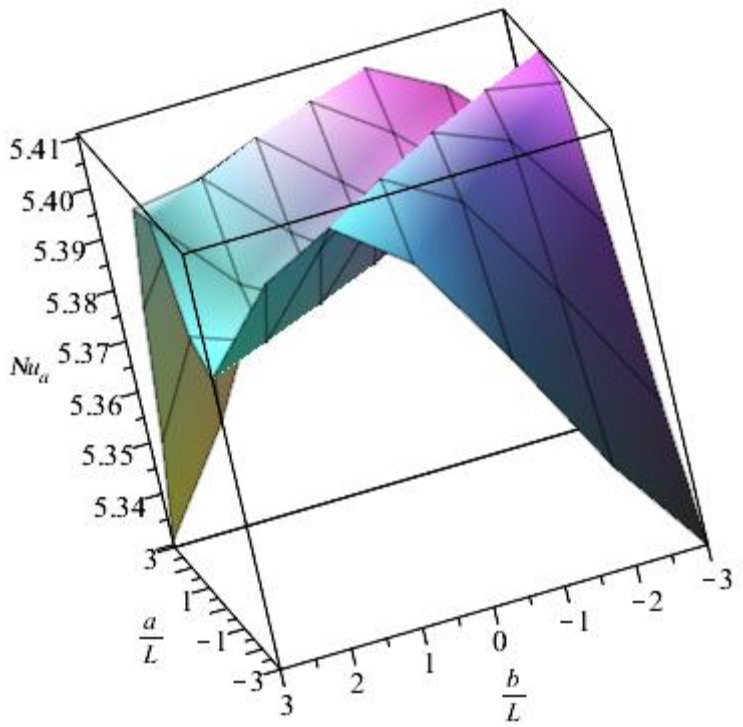

Fig. 3: The average Nusselt number Nu_a as a function of the coefficients $\frac{a}{L}$ and $\frac{b}{L}$.

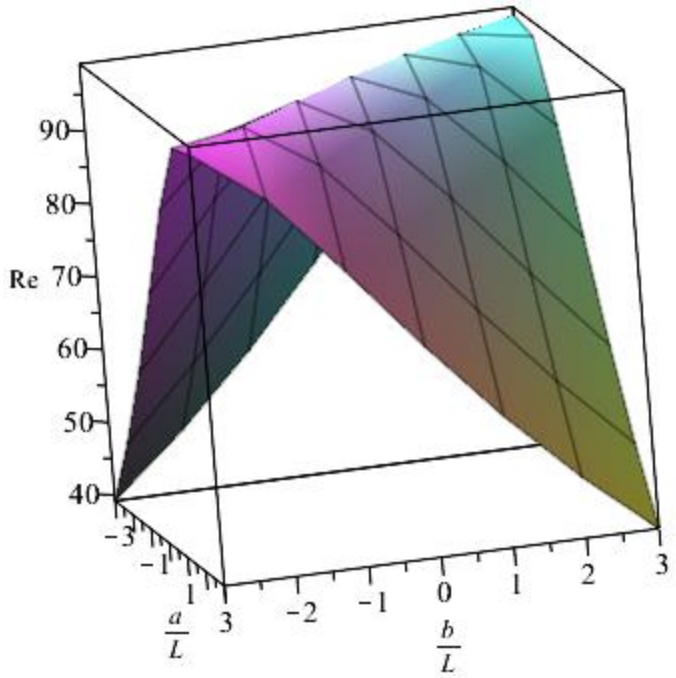

Fig. 4: The Reynolds number Re as a function of the coefficients $\frac{a}{L}$ and $\frac{b}{L}$.

A correlation for the average Nusselt number as a function of the Reynolds number can be established from the results presented in Figures 3 and 4 which represent the results in the 49 profiles. This correlation is written as:

$$Nu_a = 4.857 - 0.05037Re^{1.0628} + 0.08636Re^{0.9622} \tag{27}$$

The average Nusselt number in the case of a channel with parallel flat walls, where one wall is insulated and uniform heat flux is imposed on the other wall, is in good agreement with the value of 3.385 presented in the literature [10]. The flat walls correspond to the case where $a = b = 0$.

4. Conclusion

In this paper, Python is used for the automation of Ansys Fluent for the study of fluid flow and heat transfer in corrugated channels. The presented automation procedure is not limited only to Ansys Fluent and it can be used for all the products of Ansys which cover a variety of fields in science and engineering. The proposed automation procedure makes the optimization studies using CFD software such as Ansys Fluent more flexible where data from the simulations can be accessed through a programming language such as Python and optimum parameters can be found by implementing optimization algorithms as well as running simulations automatically for inputs that are not known for the user at the start and found iteratively. Ansys uses the IronPython version as Python.

The average Nusselt number and the Reynolds number were plotted as a function of two coefficients that define the corrugated profile. It was found that increasing the length of the upper wall decreases the Reynolds number and the average Nusselt number except for certain optimal parameters where the average Nusselt number is higher than that of parallel flat walls which is due to the development of secondary flows that brings cooler and hotter chunks of the fluid into contact leading to higher rates of conduction in a larger number of sites in the fluid. Many researchers investigated the effect of the corrugation on the heated wall however as can be seen from the results of this paper, the insulated wall also can play a significant role in heat transfer enhancement which can be of importance in heat exchanger design optimization.

Acknowledgements

This work is done with the financial support of the National Center for Scientific and Technical Research (CNRST).

References

[1] W. M. Kays and A. L. London, *Compact Heat Exchangers*. 3d Ed., McGraw Hill: New York, 1984.
[2] R. K. Shah and D. P. Sekulić, *Fundamentals of Heat Exchanger Design*. John Wiley & Sons, 2003.
[3] R. K. Shah, B. Thonon, D. M. Benforado, "Opportunities for heat exchanger applications in environmental systems," *Appl. Therm. Eng*., vol. 20, no. 7, pp. 631-650, 2000. https://doi.org/10.1016/S1359-4311(99)00045-9
[4] A. C. Caputo, P. M. Pelagagge, P. Salini, "Heat exchanger design based on economic optimisation," *Appl. Therm. Eng*., vol. 28, no. 10, pp. 1151-1159, 2008. https://doi.org/10.1016/j.applthermaleng.2007.08.010
[5] J. H. Doo, M. Y. Ha, J. K. Min, R. Stieger, A. Rolt, C. Son, "An investigation of cross-corrugated heat exchanger primary surfaces for advanced intercooled-cycle aero engines (Part-I: Novel geometry of primary surface)," *Int. J. Heat Mass Transfer*, vol. 55, no. 19-20, pp. 5256-5267, 2012. https://doi.org/10.1016/j.ijheatmasstransfer.2012.05.034
[6] J. H. Doo, M. Y. Ha, J. K. Min, R. Stieger, A. Rolt, C. Son, "An investigation of cross-corrugated heat exchanger primary surfaces for advanced intercooled-cycle aero engines (Part-II: Design optimization of primary surface)," *Int. J*. Heat Mass Transfer, vol. 61, pp. 138-148, 2013. https://doi.org/10.1016/j.ijheatmasstransfer.2013.01.084
[7] M. Bahiraei, R. Rahmani, A. Yaghoobi, E. Khodabandeh, R. Mashayekhi, M. Amani, "Recent research contributions concerning use of nanofluids in heat exchangers: A critical review," *Appl. Therm. Eng*., vol. 133, pp. 137-159, 2018. https://doi.org/10.1016/j.applthermaleng.2018.01.041
[8] T. Alam, M. H. Kim, "A comprehensive review on single phase heat transfer enhancement techniques in heat exchanger applications," *Renew. Sust. Energ. Rev*., vol. 81, no. 1, pp. 813-839, 2018. https://doi.org/10.1016/j.rser.2017.08.060
[9] G. Wang, S. P. Vanka, "Convective heat transfer in periodic wavy passages," *Int. J*. Heat Mass Transfer, vol. 38, no. 17, pp. 3219-3230, 1995. https://doi.org/10.1016/0017-9310(95)00051-A
[10] G. Fabbri, "Heat transfer optimization in corrugated wall channels," *Int. J. Heat Mass Transfer*, vol. 43, no. 23, pp. 4299-4310, 2000. https://doi.org/10.1016/S0017-9310(00)00054-5
[11] G. Fabbri, R. Rossi, "Analysis of the heat transfer in the entrance region of optimised corrugated wall channel," *Int. Commun. Heat Mass Transfer*, vol. 32, no. 7, pp. 902-912, 2005. https://doi.org/10.1016/j.icheatmasstransfer.2004.08.027
[12] P. Naphon, "Effect of wavy plate geometry configurations on the temperature and flow distributions," *Int. Commun. Heat Mass Transfer*, vol. 36, no. 9, pp. 942-946, 2009. https://doi.org/10.1016/j.icheatmasstransfer.2009.05.007
[13] N. Kurtulmuş, B. Sahin, "A review of hydrodynamics and heat transfer through corrugated channels," *Int. Commun. Heat Mass Transfer*, vol. 108, 104307, 2019. https://doi.org/10.1016/j.icheatmasstransfer.2019.104307